Asian Journal of Andrology (2023) 25, 389–397
www.asiaandro.com; www.ajandrology.com

Open Access

ORIGINAL ARTICLE

Male Health

Testicular exosomes disturb the immunosuppressive phenotype of testicular macrophages mediated by miR-155-5p in uropathogenic *Escherichia coli*-induced orchitis

Jia Xu, Chao He, Yi-Wei Fang, Zhi-Yong Hu, Mei-Lin Peng, Yuan-Yao Chen, Yu-Fang Su, Chun-Yan Liu, Hui-Ping Zhang, Kai Zhao

Male reproductive infections are known to shape the immunological homeostasis of the testes, leading to male infertility. However, the specific pathogenesis of these changes remains poorly understood. Exosomes released in the inflammatory microenvironment are important in communication between the local microenvironment and recipient cells. Here, we aim to identify the immunomodulatory properties of inflammatory testes-derived exosomes (IT-exos) and explore their underlying mechanisms in orchitis. IT-exos were isolated using a uropathogenic *Escherichia coli* (UPEC)-induced orchitis model and confirmed that IT-exos promoted proinflammatory M1 activation with increasing expression of tumor necrosis factor-α (TNF-α), interleukin-1β (IL-1β), and interleukin-6 (IL-6) *in vitro*. We further used small RNA sequencing to identify the differential miRNA profiles in exosomes and primary testicular macrophages (TMs) from normal and UPEC-infected testes, respectively, and identified that miR-155-5p was highly enriched in IT-exos and TMs from inflammatory testes. Further study of bone marrow derived macrophages (BMDMs) transfected with miR-155-5p mimic showed that macrophages polarized to proinflammatory phenotype. In addition, the mice that were administrated IT-exos showed remarkable activation of TM1-like macrophages; however, IT-exos with silencing miR-155-5p showed a decrease in proinflammatory responses. Overall, we demonstrate that miR-155-5p delivered by IT-exos plays an important role in the activation of TM1 in UPEC-induced orchitis. Our study provides a new perspective on the immunological mechanisms underlying inflammation-related male infertility.
Asian Journal of Andrology (2023) **25**, 389–397; doi: 10.4103/aja202243; published online: 29 July 2022

Keywords: male infertility; miR-155-5p; orchitis; testicular exosome; testicular macrophage polarization

INTRODUCTION

Poor sperm quality and male infertility are challenges in the field of reproductive medicine.[1] Infections and inflammation in the genital tract account for 15% of all cases of male fertility disorders; however, there is no sufficient knowledge of the potential pathology, consistent diagnostic criteria or timely effective clinical treatments in the clinic.[2,3] The testis is regarded as an immune-privileged organ that tolerates germ cell neoantigens and maintains immune homeostasis.[4,5] Orchitis, which disturbs testicular immune homeostasis, is characterized by an overwhelming and uncontrolled inflammatory response with massive infiltration of inflammatory cells, testicular damage, and subsequent infertility;[6] however, the underlying mechanisms contributing to disturbing testicular immune homeostasis in male fertility disorders are largely unknown.

Inflammation is a basic biological process for maintaining immune homeostasis in the body. Macrophages, as effectors and regulators of the inflammatory cascade, are involved in the promotion of adaptive immune responses. Polarization of macrophages, such as classical activated macrophages (M1) and alternatively activated macrophages (M2), is the key to completing these functions.[7] Generally, M1 macrophages are usually induced by Th1-type cytokines and play a major role in antibacterial and proinflammatory properties, while M2 macrophages are stimulated by Th2-type cytokines and have anti-inflammatory properties. Testicular macrophages (TMs), which represent the predominant population of immune cells in the testis, also maintain testicular immune privilege by skewing the innate immune response.[4,8–10] Under physiological conditions, TMs exhibit an M2-like immunosuppressive state by secreting high levels of the anti-inflammatory cytokine interleukin-10 (IL-10) and only low amounts of proinflammatory cytokines, such as tumor necrosis factor-α (TNF-α) and IL-6.[4,11,12] However, during testis inflammation, the number of proinflammatory TM1 increases with an increased level of TM1-derived proinflammatory cytokines TNF-α, IL-1β, and IL-1α,[13–15] which ultimately disrupt testicular immune privilege and impair spermatogenesis and steroidogenesis.[16] However, the underlying mechanisms by which orchitis activates TM1 and disrupts testicular immune privilege remain poorly understood and are becoming a new hotspot in the field of male infertility.

Institute of Reproductive Health, Center for Reproductive Medicine, Tongji Medical College, Huazhong University of Science and Technology, Wuhan 430030, China.
Correspondence: Dr. HP Zhang (zhpmed@126.com) or Dr. K Zhao (kai_zhao@hust.edu.cn)
Received: 09 March 2022; Accepted: 28 May 2022

Exosomes are secreted by living cells and are characterized as vesicles 30–150 nm in diameter with lipid double-layered membrane structures bearing functional proteins, lipids, and noncoding RNAs. Exosomes mediate cell-to-cell communication by transmitting microenvironmental signals in various biological processes and diseases.[17,18] Accumulating evidence has revealed their function in inflammation regulation and identified their critical role in the development of various diseases by regulating the polarization of macrophages.[19–21] A number of studies have focused on the function of extracellular noncoding RNAs, especially microRNAs (miRNAs), encapsulated and transferred by exosomes, as they are stable and have regulatory abilities by targeting gene expression at posttranscriptional level in recipient cells.[21,22] It has been reported that visceral adipose tissue-derived exosomes exacerbate colitis severity and promote macrophage M1 polarization by transferring proinflammatory miR-155-5p.[20] In addition, it is worth noting that most studies on the male reproductive system have focused on epididymosomes and prostasomes in the seminal fluid;[23–26] however, the number of studies on testes-derived exosomes remains limited. More importantly, the roles of testicular exosomes and testicular exosome-derived miRNAs during orchitis are also poorly understood.

In the present study, we successfully isolated testicular exosomes and investigated the role of testes-derived exosomes (IT-exos) in regulating the activation of M1 macrophages; we further used small RNA sequencing to identify the differential miRNA profiles in testicular exosomes and primary TMs from normal and uropathogenic *Escherichia coli* (UPEC)-infected testes. We found that miR-155-5p enriched in IT-exos can promote the activation of proinflammatory macrophages during UPEC-induced orchitis. Our findings provide a new perspective for the immunological mechanisms underlying inflammation-related male infertility.

MATERIALS AND METHODS

Animals and treatments

Wild-type C57BL/6J male mice (8–9 weeks of age) were purchased from the animal center of Tongji Medical College, Huazhong University of Science and Technology (Wuhan, China). The animals were kept in a specific-pathogen-free (SPF) room with constant temperature and light (12 h light-dark cycle) and fed standard food and water. All animal experiments were performed in strict accordance with the approved guidelines from the Institutional Animal Care and Use Committee of Tongji Medical College (No. IEC-S235).

UPEC-CFT073 (NCBI: AE014075, NC_004431) characterized by Welch *et al.*[27] was used to establish UPEC-induced experimental orchitis in male mice as previously described,[28] and some adjustments were made in this study. Briefly, under isoflurane anesthesia, approximately 5–10 μl of UPEC suspension (5×10^5 bacteria) was injected bilaterally into the vas deferens proximal to the cauda epididymis using 30 G needles (Gaoge, Shanghai, China). Sham operated mice were injected with an equal volume of saline. Ligation was performed close to the injection site to prevent the spread of infection.

Testicular histopathology

Mouse testes were collected for further detection 7 days after treatment. For the histopathological assessment, the testes were removed, fixed in 4% paraformaldehyde (Servicebio, Wuhan, China) at 4°C overnight, and then embedded in paraffin. Then, the continuous testicular paraffin sections were treated with dewaxed xylene, rehydrated in gradient alcohol, and stained with hematoxylin-eosin (H&E; Servicebio) to detect testicular histopathology.

Immunofluorescence staining

The testes were collected and fixed in 4% paraformaldehyde and then embedded in paraffin. Testes sections (5 μm) were then dewaxed with xylene and hydrated with ethanol. After antigen retrieval, the slides were placed in 3% hydrogen peroxide solution (25 min at room temperature) to block endogenous peroxidase and then blocked with 3% bovine serum albumin (BSA). Then, the expression of F4/80 was detected by incubating with rabbit anti-F4/80 antibody (1:500; GB11027, Servicebio) at 4°C overnight. After 3 washes with phosphate buffered solution (PBS; Biosharp, Hefei, China), fluorescein isothiocyanate (FITC) conjugated goat anti-rabbit secondary antibodies (1:200; GB22303, Servicebio) were incubated at room temperature in the dark for 1 h. After 4',6-diamidino-2-phenylindole (DAPI; Servicebio) staining, fluorescence images were captured under a fluorescence microscope Leica SP8 (Leica, Wetzlar, Germany). For F4/80 positive staining quantification analysis, five fields of each section were randomly selected to count the number of $F4/80^+$ cells at ×400 using ImageJ software (National Institutes of Health, Bethesda, MD, USA). Then, the average number of positive cells per field in each section was calculated. Three independent experiments were performed for statistical analysis.

Cell culture and treatments

Murine bone marrow derived macrophages (BMDMs) were isolated and cultivated as previously described.[15,29] Briefly, the bone marrow from C57BL/6J mice was flushed into cold PBS with a 1-ml syringe, passed through a 70-μm strainer, and centrifuged (Heal Force, Shanghai, China) at 500*g* for 5 min at 4°C. The cell pellet was resuspended in 2 ml red blood cell lysis buffer for 1–3 min to remove the erythrocytes, resuspended again in Roswell Park Memorial Institute-1640 (RPMI-1640; Gibco, Carlsbad, CA, USA) medium, including 10% fatal bovine serum (FBS; Gibco) and 1% penicillin/streptomycin (BioFroxx, Guangzhou, China), and then centrifuged (Heal Force) at 500*g* for 5 min at 4°C. The concentration of bone marrow cells was adjusted to 2×10^6 cells per ml and seeded onto 6-well plates. The cells were cultured with RPMI-1640 medium supplemented with 10% FBS, 1% penicillin/streptomycin, and 50 ng ml^{-1} murine macrophage-colony stimulating factor (M-CSF; PeproTech, Rocky Hill, NJ, USA) for 6 days, and fresh medium was added every 3 days. For BMDM-M1 activation, BMDMs were stimulated in RPMI-1640 medium containing 10% FBS, 100 ng ml^{-1} lipopolysaccharide (LPS; PeproTech) and 50 ng ml^{-1} interferon-γ (IFN-γ; PeproTech) for 24 h or 48 h. For transfection, BMDMs were seeded in glass cover slides or cell plates. Lipofectamine 3000 Reagent (Invitrogen, Carlsbad, CA, USA) was used according to the manufacturer's protocol. The miR-155-5p mimic and miRNA-NC were synthesized by GenePharma (Shanghai, China).

Primary TMs were isolated as previously described.[28,30,31] Briefly, the testes were removed from 8–9 weeks C57BL/6J mice, washed with pre-cold PBS, and then decapsulated and digested in Dulbecco's modified Eagle's medium/F-12 medium (DMEM/F-12; Gibco) containing collagenase I (1 mg ml^{-1}, Sigma, Louis, MO, USA) and DNase I (60 U ml^{-1}, Sigma) at 34°C for 15 min. Then, the digestive solution was filtered to separate the interstitial cells and seminiferous tubules. After centrifugation of the suspension, the pellet containing interstitial cells was resuspended and purified with a discontinuous density percoll solution (GE Healthcare, Uppsala, Sweden). After centrifugation, the relevant interphase containing immune cells was collected and washed with PBS, and a single-cell suspension of testicular interstitial immune cells was obtained. Next, these cells were counted, resuspended in 1 ml autoMACS running buffer

(Miltenyi, Bergisch Gladbach, Germany), and incubated with anti-F4/80-MicroBeads (Miltenyi) for 15 min at 4°C according to the manufacturer's instructions. After washing, the cellular suspension was loaded into the LS separation column and attached to a MACS separator (Miltenyi). The magnetically labeled cells ($F4/80^+$ macrophages) were flushed immediately by pushing the plunger into the column. The purity of TMs was determined through flow cytometry by incubating with eFluor450-F4/80 (48-4801-82, eBioscience, Waltham, MA, USA). The purity of TMs (n = 4 per group) was approximately 83% (**Supplementary Figure 1**).

Flow cytometry

To detect the phenotype of TMs, testicular interstitial immune cells were incubated with flow cytometry antibodies, including FVS520 (564407, BD Biosciences, Franklin Lakes, NJ, USA), PE-F4/80 (565410, BD Biosciences), PerCP-Cy5.5-CD11b (550993, BD Biosciences), and PE-Cy7-CD86 (560582, BD Biosciences) at 4°C in the dark for 30 min. The cells were washed with PBS buffer containing 1% BSA, fixed, permeabilized, and then incubated with Alexa Fluor 647-CD206 (565250, BD Biosciences) for 30 min on ice. After that, the cells were washed and resuspended in washing buffer. Flow cytometry was performed on Agilent novoCyte (Agilent Technologies, Santa Clara, CA, USA). The fluorescence minus one (FMO) control and single staining fluorescence control of each fluorescent marker was used to assist the flow cytometry gating strategy (**Supplementary Figure 2**).

Testicular exosome isolation and identification

Testicular exosome isolation was performed using differential centrifugation as previously described.[32] Briefly, the testes were removed and washed with pre-cold PBS and digested in DMEM buffer containing 1 mg ml^{-1} collagenase I (Sigma), 60 U ml^{-1} DNase I (Sigma) and 10% free-exosome FBS at 37°C for 30 min at 15*g*. Then the resulting digestive solution was treated by differential centrifugation. First, the samples were centrifuged (Heal Force) at 300*g* for 10 min at 4°C followed by 2000*g* for 20 min at 4°C to remove the cells, and the debris was discarded. Then, the supernatant was used for the next centrifugation (16 500*g*, 20 min, 4°C) to remove large vesicles. Next, the supernatant was ultracentrifuged at 118 000*g* for 2.5 h at 4°C to pellet all testicular exosomes (Optima L-100XP Ultracentrifuge, Beckman Coulter, Brea, CA, USA). After one wash with PBS, the exosomes were obtained and resuspended in PBS or other medium for further research.

The freshly isolated testicular exosomes were fixed with 2.5% glutaraldehyde stationary liquid, loaded onto 200-mesh carbon-coated formvar grids for 5 min, and then stained with 2% phosphotungstic acid for 5 min at room temperature. Exosome images were captured using a transmission electron microscope (TEM; HT7700, Hitachi, Tokyo, Japan).

The particle size and concentration of the testicular exosomes were tested using the ZetaView NTA technique by Particle Metrix (PMX Group, Meerbusch, Germany).

Exosome take up assay

Fresh exosomes were incubated with 10 μmol l^{-1} lipophilic dye PKH26 (Sigma) according to the manufacturer's protocol. PKH26-labelled exosomes were cocultured with BMDMs for 24 h. Cells were washed with PBS and then fixed with 4% paraformaldehyde for 15 min. After DAPI staining, confocal images were obtained using a Leica SP8 System (Leica).

Bioluminescence imaging in vivo

IT-exos were prestained with the liposomal dye PKH26 (Sigma) according to the manufacturer's instructions. PKH26-labelled exosomes were injected into the testis as previously described.[33] Briefly, adult mice (8–9 weeks old, n = 3) were under general anesthesia with isoflurane, and then approximately 10 μl of PKH26-labelled exosomes (1 μg $μl^{-1}$ at the protein level) was injected bilaterally into the testis. Sham-operated mice were injected with an equal volume of unlabelled exosomes. The testes were removed 24 h later. Bioluminescence imaging was performed using an *in vivo* imaging system (Bruker, Karlsruhe, Germany).

miRNA loading into testicular exosomes

Testicular exosomes and antagomiR-155 or negative control (GenePharma) were mixed in electroporation buffer (1.15 mmol l^{-1} potassium phosphate pH 7.2, 25 mmol l^{-1} potassium chloride, and 21% OptiPrep) at 350 V/150 mF in 0.4 cm electroporation cuvettes, as previously described.[20,34] After electroporation, exosomes were washed with PBS, followed by another round of exosome isolation with ultracentrifugation. Then, the exosomes were resuspended in PBS, kept on ice and injected into the mice every 48 h (4 times total). For each injection, approximately 10 μl of exosomes (1 μg $μl^{-1}$ at the protein level) was bilaterally injected into the testis. On day 7, testes were collected for further detection.

Real-time quantitative polymerase chain reaction (RT-qPCR)

The total RNA of BMDMs, TMs, and testes was extracted with the miRNeasy Mini Kit (217004, Qiagen, Dusseldorf, Germany). For mRNA, total RNA was transcribed into complementary DNAs (cDNAs) using the PrimeScript RT reagent kit (11141ES60, Yeasen, Shanghai, China). For miRNA, reverse transcription was performed using the microRNA Reverse Transcription Kit (RR047A, TaKaRa, Tokyo, Japan). RT-qPCR was performed according to the protocol of SYBR Green MasterMix (Yeasen 11201, Yeasen). The miRNA and mRNA levels were normalized to U6 or glyceraldehyde-3-phosphate dehydrogenase (*GAPDH*), respectively. The relative expression of these RNAs was calculated using the $2^{-\Delta\Delta CT}$ method. All the primers used in the study are listed in **Supplementary Table 1.**

Small RNA sequencing

Total RNA of testicular exosomes and primary testicular macrophages was isolated using the miRNeasy Mini Kit (217004, Qiagen). Three duplicate samples for each treatment were included. The small RNA sequencing service was provided by Wuhan Bioacme Biotechnology Co., Ltd. (Wuhan, China) and the library products were sequenced with the Illumina HiSeq-SE50 platform. The read statistics of miRNAs are listed in **Supplementary Table 2–4**.

Enzyme linked immunosorbent assay (ELISA)

The testis was removed, washed with pre-cold PBS, cut into small pieces and placed in pre-cold lysis buffer (IS007, Cloud-Clone Corp., Wuhan, China) according to the instructions (1 ml lysis buffer supplemented with 50 mg tissue). Then, ultrasonic treatment was performed for clarification. After centrifuge (10 000*g*, 5 min), testicular tissue homogenization was obtained. Testicular tissue homogenization was used to detect the protein levels of IL-1β (SEA563Mu, Cloud-Clone Corp.), TNF-α (SEA133Mu, Cloud-Clone Corp.), and IL-10 (SEA056Mu, Cloud-Clone Corp.). The methods were determined with specific ELISA kits according to the manufacturer's directions.

Western blot

Western blot assays were performed using routine protocols. Protein extracted from testicular exosomes and testis tissue was separated by 10% sodium dodecyl sulfate-polyacrylamide gels (P0012AC, Beyotime)

and transferred to 0.45 μm polyvinylidene fluoride (PVDF) membranes. Then, the cells were blocked with 5% nonfat milk for 1 h at room temperature, and incubated at 4°C overnight with primary antibodies specific for Alix (1:1000; 92880S, CST, Beverly, MA, USA), CD63 (1:1000; ab271286, Abcam, Cambridge, UK), CD81 (1:1000; 56039) and Calnexin (1:20 000; 10427-2-AP, Proteintech, Rosemont, IL, USA). Then, the membranes were washed and incubated with horseradish peroxidase (HRP)-goat anti-rabbit secondary antibodies (1:50 000; BL003A, Biosharp) or HRP-goat anti-mouse secondary antibodies (1:50 000; BL001A, Biosharp). The blots were detected by enhanced chemiluminescence (SQ201, Omni-ECL, Shanghai, China) and quantified using the Bio-Rad imaging system (Bio Rad, Hercules, CA, USA).

Statistical analyses

Data was shown as the mean ± standard error of mean (s.e.m.). Student's *t* test was applied for the comparison of two groups. Multiple group comparisons were performed using one-way analysis of variance (ANOVA), followed by Tukey's multiple comparisons test. GraphPad Prism 8.0 (GraphPad Software, San Diego, CA, USA) was used for all data analyses. $P < 0.05$ was considered statistically significant.

RESULTS

The immunosuppressive phenotype of TMs is disturbed after UPEC-induced orchitis in mice

To explore the polarization of TMs in UPEC-induced orchitis, a mouse model was applied according to our previous study.[28] Seven days after UPEC infection, H&E staining showed that the testes were characterized by increased interstitial cells and loss of germ cells in the seminiferous tubules, compared to the control group (**Figure 1a**). Given that immune cells mainly exist in the interstitium of the testis and TMs are the largest number of immune cells in the testis,[8] we detected F4/80$^+$ macrophages after UPEC infection in the testis (**Figure 1b** and **1c**). Massive F4/80$^+$ macrophages infiltrated the interstitium of the UPEC-infected testis. Next, we evaluated proinflammatory TM1 and anti-inflammatory TM2 markers in primary TMs. As shown in **Figure 1d**, the flow cytometry data also showed that UPEC infection significantly increased ($P < 0.01$) the number of F4/80$^+$CD11b$^+$ TMs in the testis (**Figure 1d** and **1e**). We then examined M1 and M2 marker expression in TMs, and found that the percentage of CD206$^+$ TM2 in F4/80$^+$CD11b$^+$ TMs was significantly decreased but the percentage of CD86$^+$ TM1 in F4/80$^+$CD11b$^+$ TMs was significantly increased ($P < 0.01$) in the UPEC treatment group (**Figure 1d**–**1g**). Collectively, these data suggest the polarization of TMs toward proinflammatory TM1 in UPEC-induced orchitis. We hypothesized that the increase in proinflammatory TM1 disturbs the immunosuppressive phenotype of the testis in the early stage of UPEC-induced orchitis, which may play an important role in inflammation-related testis damage.

Exosomes from inflammatory testes govern the phenotypic switch of BMDMs to the proinflammatory M1 phenotype

Accumulating studies suggest that local microenvironmental signals govern the phenotypic switch of macrophages.[35,36] Exosomes, as media for cell-to-cell communication in the microenvironment, have been reported to induce proinflammatory macrophage activation by transferring inflammatory signals.[19,37] Therefore, we next sought to determine whether IT-exos enhanced inflammation and initiated the polarization of TM1. First, we isolated control testes-derived exosomes (CT-exos) and IT-exos. TEM showed that CT-exos and IT-exos had the same typical saucer-like morphology with an average size of approximately 100 nm in diameter (**Figure 2a**). As in a previous study,[32] nanoparticle tracking analysis confirmed that the size of these exosomes was approximately 100–150 nm in diameter (**Figure 2b**). To determine the characterization in advance, we detected typical exosome markers by western blot. The results showed that the exosome markers Alix, CD63 and CD81 were highly expressed in these exosomes while the endoplasmic reticulum marker Calnexin, as the negative exosome marker, was expressed at low levels in testicular exosomes (**Figure 2c**), indicating that testicular exosomes had been successfully collected from the supernatant of tissue digestive fluid. To investigate the effects of IT-exos on macrophage function, BMDMs were isolated and cocultured with IT-exos. PKH-26-labeled (red) IT-exos were within the cytoplasm, indicating that IT-exos were internalized by BMDMs (**Figure 2d**). Next, we evaluated M1 and M2 markers in BMDMs that were stimulated with PBS, CT-exos, and IT-exos for 48 h using RT-qPCR (**Figure 2e**). The data showed that the mRNA levels of proinflammatory M1-related genes, such as *TNF-α*, *IL-1β*, and *IL-6*, were significantly increased ($P < 0.01$) in IT-exos-stimulated cells, compared with PBS control or CT-exos-treated cells (**Figure 2f**). However, the level of anti-inflammatory M2-related gene, such as *IL-10*, was decreased ($P < 0.05$) in BMDMs after coculturing with IT-exos (**Figure 2f**). These results suggest that IT-exos have proinflammatory properties and promote the polarization of TMs toward proinflammatory TM1.

The differentially expressed miRNAs of testicular exosomes and primary TMs in UPEC-induced orchitis

To elucidate the underlying mechanisms by which IT-exos promote the polarization of TMs to proinflammatory TM1, small RNA sequencing was performed to analyze the differentially expressed miRNAs in CT-exos and IT-exos. The sequencing data showed differentially expressed miRNAs in testicular exosomes from the control group and UPEC group. We identified 54 upregulated and 3 downregulated miRNAs in IT-exos. Furthermore, the volcano plot and heatmap show the highly enriched miRNAs in IT-exos (**Figure 3a**, **3b**, and **Supplementary Table 2**). A recent study reported that the miRNAs that are transferred to recipient cells by exosomes are not random and may vary due to the different types of recipient cells.[38] Therefore, we also analyzed differentially expressed miRNAs in primary TMs from the control group and UPEC-infected group using small RNA sequencing. The results showed that there were 31 upregulated and 26 downregulated miRNAs in these primary TMs derived from UPEC-infected testes (**Figure 3c**, **3d**, and **Supplementary Table 3**). Then, a Venn diagram was used to identify overlapping with-group miRNAs (**Figure 3e** and **Supplementary Table 4**). The results showed that 17 miRNAs were shared in both databases, suggesting that these IT-exos-associated miRNAs were highly relevant to the polarization of TMs to proinflammatory TM1. Among these miRNAs, we found that there were some miRNAs associated with immune regulation, including mmu-miR-155-5p, mmu-miR-146b-5p, mmu-miR-146a-5p, mmu-miR-21a-3p, mmu-miR-223-3p, mmu-miR-21a-5p, and mmu-miR-142a-3p.

IT-exos-derived miR-155-5p facilitates macrophage polarization toward the proinflammatory phenotype

According to the sequencing data, miR-155-5p was one of the most highly expressed both in IT-exos and in primary TMs derived from UPEC-infected testes. Therefore, we focused on miR-155-5p, which was also reported to be related to macrophage polarization.[19,39,40] To confirm the sequencing results, we evaluated the expression

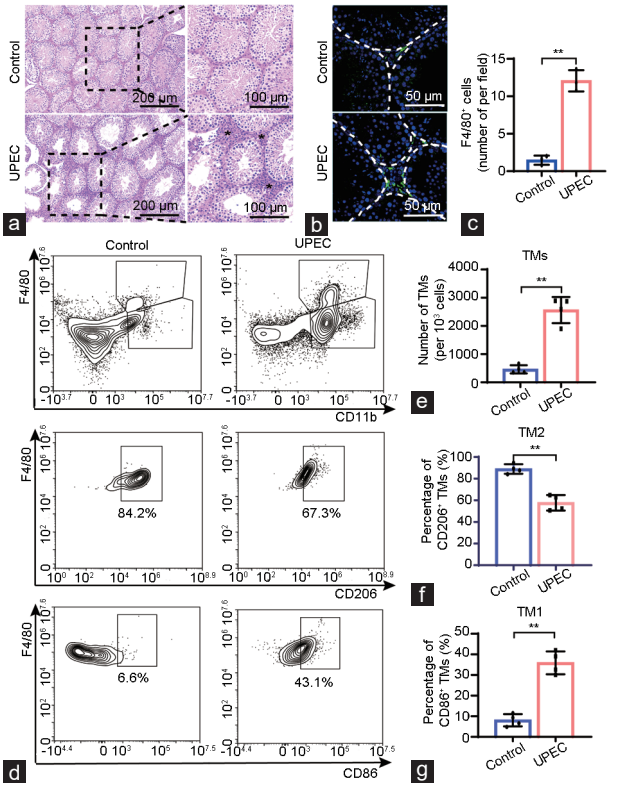

Figure 1: The immunosuppressive phenotype of TMs is disturbed after UPEC-induced orchitis in mice. (**a**) Testicular tissue sections from each treatment group were stained with hematoxylin and eosin. Scale bars = 200 μm (left), and scale bars = 100 μm (right). (**b**) Representative immunofluorescence image of F4/80$^+$ TM cells (green) in each treatment group. Scale bars = 50 μm. (**c**) Quantification of F4/80$^+$ TM cells (numbers of per field, n = 3). (**d**) Representative flow cytometry plots of F4/80$^+$CD11b$^+$ TMs (upper panel), F4/80$^+$CD11b$^+$CD206$^+$ TM2 (middle panel), and F4/80$^+$CD11b$^+$CD86$^+$ TM1 (lower panel) in the testes of different groups are presented. (**e**) The number of F4/80$^+$CD11b$^+$ macrophages in the testes of different groups is presented (n = 4 for each group). The percentage of (**f**) CD206$^+$ TM2 and (**g**) CD86$^+$ TM1 cells among F4/80$^+$CD11b$^+$ TMs in different groups are shown, respectively (n = 4 for each group). All results are presented as the mean ± s.e.m. $^*P < 0.05$, $^{**}P < 0.01$. s.e.m.: standard error of mean; TM: testicular macrophage; UPEC: uropathogenic *Escherichia coli*.

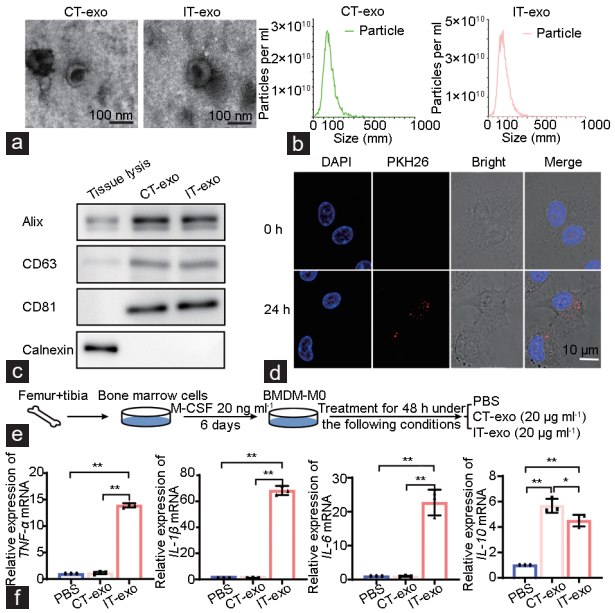

Figure 2: Exosomes from inflammatory testes govern the phenotypic switch of BMDMs to the proinflammatory M1 phenotype. (**a**) Representative TEM image of CT-exo or IT-exo. Scale bars = 100 nm. (**b**) The particle size distribution of testicular exosomes (CT-exo or IT-exo) was measured by NTA. (**c**) Western blotting of testicular exosomes (CT-exo or IT-exo), including three typical exosomal markers (Alix, CD63 and CD81) and the endoplasmic reticulum marker Calnexin as the negative exosome marker. (**d**) Confocal images showing BMDM uptake PKH-26-labelled IT-exos (red) after co-culturing for 24 h. Scale bar = 10 μm. (**e**) The flowchart of BMDMs polarized by testicular exosomes (exosomes 20 μg ml^{-1} or an equal volume of PBS as a negative control). (**f**) The mRNA levels of M1-related genes (*TNF-α*, *IL-1β*, and *IL-6*) and an M2-related gene (*IL-10*) in BMDMs after co-culturing with different testicular exosomes for 48 h (n = 3). All results are presented as the mean ± s.e.m. $^*P < 0.05$, $^{**}P < 0.01$. s.e.m.: standard error of mean; BMDM: bone marrow derived macrophage; TEM: transmission electron microscope; DAPI: 4',6-diamidino-2-phenylindole; CT-exo: control testes-derived exosome; IT-exo: inflammatory testes-derived exosome; NTA: nanoparticle tracking analysis; PBS: phosphate buffered solution; *TNF-α*: tumor necrosis factor-α; mRNA: messenger ribonucleic acid; *IL-1β*: interleukin-1β; *IL-6*: interleukin-6; *IL-10*: interleukin-10.

level of miR-155-5p in different tissues. RT-qPCR data verified that miR-155-5p was upregulated ($P < 0.01$) in IT-exos, UPEC-infected testicular tissue, and primary TMs from UPEC-infected testes (**Figure 4a** and **4b**). In addition, we verified the expression of miR-155-5p in BMDM-derived M1 cells. The results showed that the expression level of miR-155-5p was increased ($P < 0.01$) in BMDM-derived M1 cells in a time-dependent manner (**Figure 4c**). These data suggest that miR-155-5p is related to promoting macrophage M1 polarization. Next, to identify the role of IT-exos derived miR-155-5p in macrophage polarization, BMDMs were cocultured with PBS, CT-exos, and IT-exos. The results showed that miR-155-5p was markedly increased ($P < 0.01$) in BMDMs stimulated with IT-exos compared with PBS and CT-exos (**Figure 4d**). Moreover, transfection of BMDMs with miR-155-5p mimics increased ($P < 0.01$) the expression of proinflammatory M1-related factors, such as *TNF-α*, *IL-1β*, and *IL-6*, and decreased ($P < 0.01$) the expression of the anti-inflammatory M2-related cytokine *IL-10* (**Figure 4e**). These data confirmed that IT-exos-derived miR-155-5p governs macrophage polarization to a proinflammatory phenotype.

IT-exos disturbed the immunosuppressive phenotype of TMs, which was partially reversed by antagomiR-155 in vivo

To further elucidate the effects of IT-exosomal miR-155-5p on TM polarization, *in vivo* experiments were performed. First, we confirmed that IT-exos could be retained within the testes after intratesticular injection of PKH-26-labeled IT-exos through bioluminescence (**Figure 5a**). Additionally, we found that the percentage of PKH-26$^+$ TMs was higher after intratesticular injection of PKH-26-labeled IT-exos (**Supplementary Figure 3** and **Supplementary Methods and Materials**). Therefore, the effects of IT-exos or IT-exos loaded with antagomiR-155 (IT-exo-antagomiR-155) treatment on the inflammatory response and resulting testicular tissue impairment were assessed in a murine model (**Figure 5b**).

Seven days after IT-exos injection into the testis, testes were removed, and testis sections showed that IT-exos induced a marked increase ($P < 0.01$) in testicular interstitial F4/80$^+$ TMs (**Figure 5c** and **5d**). Furthermore, we analyzed primary testicular immune cells by flow cytometry and found that IT-exos injection increased ($P < 0.01$) the number of F4/80$^+$CD11b$^+$ TMs (**Figure 5e** and **5f**) and CD86$^+$ (TM1) expression in F4/80$^+$CD11b$^+$ TMs (**Figure 5e** and **5g**) but decreased ($P < 0.01$) CD206$^+$ (TM2) expression in F4/80$^+$CD11b$^+$ TMs (**Figure 5e** and **5h**), consistent with

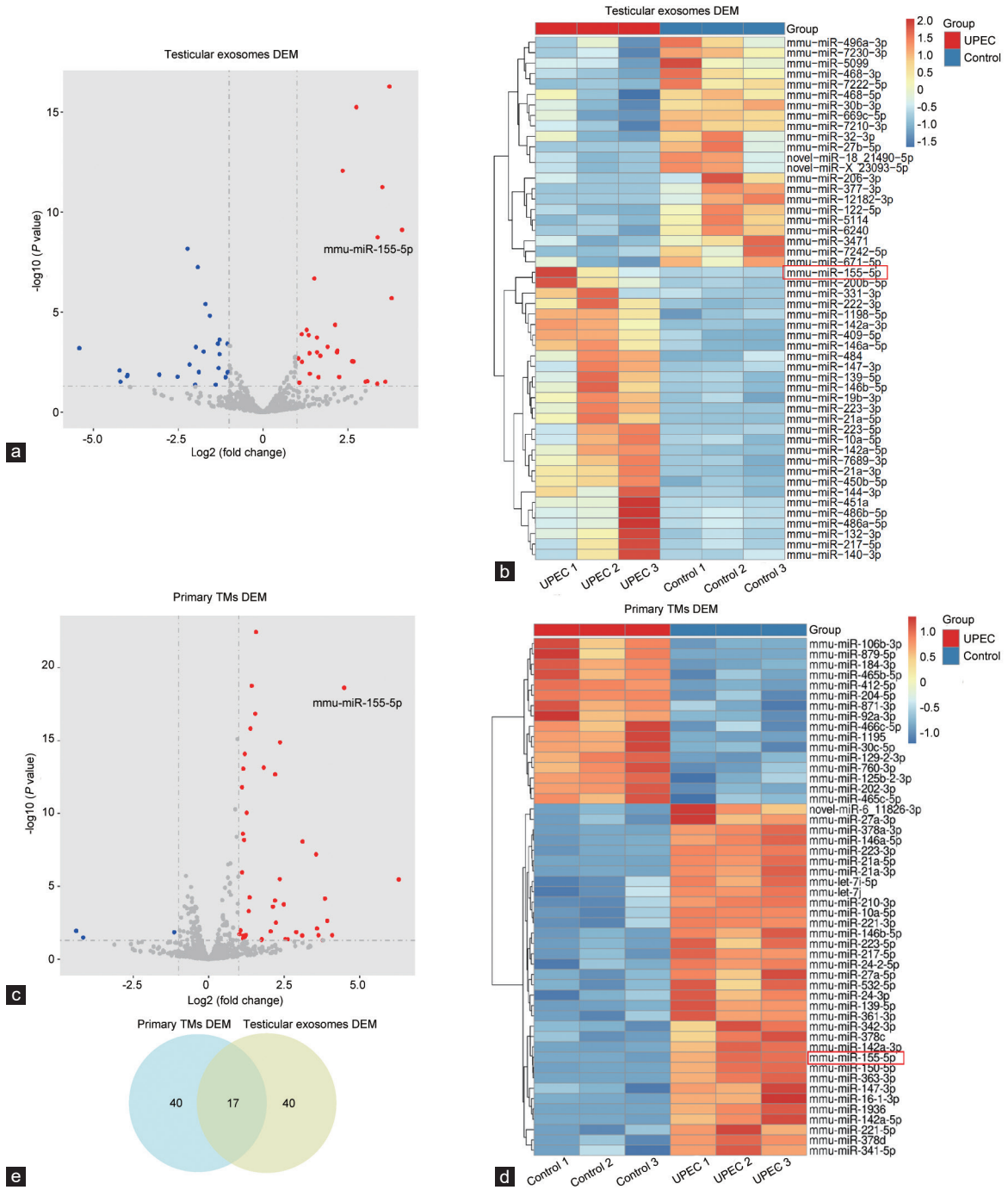

Figure 3: Differentially expressed miRNAs of primary TMs and testicular exosomes in UPEC induced orchitis. The differentially expressed miRNA profiles of testicular exosomes isolated from testes from the control group and UPEC group (8–9 weeks old, $n = 3$) of (**a**) volcano plot and (**b**) heatmap. The differentially expressed miRNA profiles of primary TMs isolated from testes from the control group and UPEC group (8–9 weeks, $n = 3$) of (**c**) volcano plot and (**d**) heatmap. (**e**) The differentially expressed miRNAs between primary TMs and testicular exosomes were analyzed by Venn diagram. miRNA: micro ribonucleic acid; DEM: differentially expressed miRNAs; TM: testicular macrophage; UPEC: uropathogenic *Escherichia coli*.

the inflammation caused by UPEC infection. However, these results were partially reversed when IT-exos loaded with antagomiR-155 were applied (**Figure 5c**–**5e**), suggesting that IT-exos have proinflammatory properties and disturbed testicular immune homeostasis *in vivo*. Moreover, we also detected proinflammatory (TNF-α and IL-1β) and anti-inflammatory cytokines (IL-10) using ELISA. The levels of TNF-α and IL-1β cytokines in the testes were significantly upregulated ($P < 0.01$) after IT-exos treatment, but the effects were reversed by the addition of antagomiR-155. Of note, the ant-inflammatory cytokine IL-10 was higher ($P < 0.01$) in the IT-exos-antagomiR-155 treatment group than that in the control group (**Figure 5i**). These data show that miR-155-5p derived from IT-exos disturbed the immunosuppressive phenotype of TMs, and the effects were partially reversed by antagomiR-155. H&E staining showed that IT-exos induced a profound increase in testicular interstitial cells but partially lost germ cells in the seminiferous tubules (**Figure 5j**), in line with the

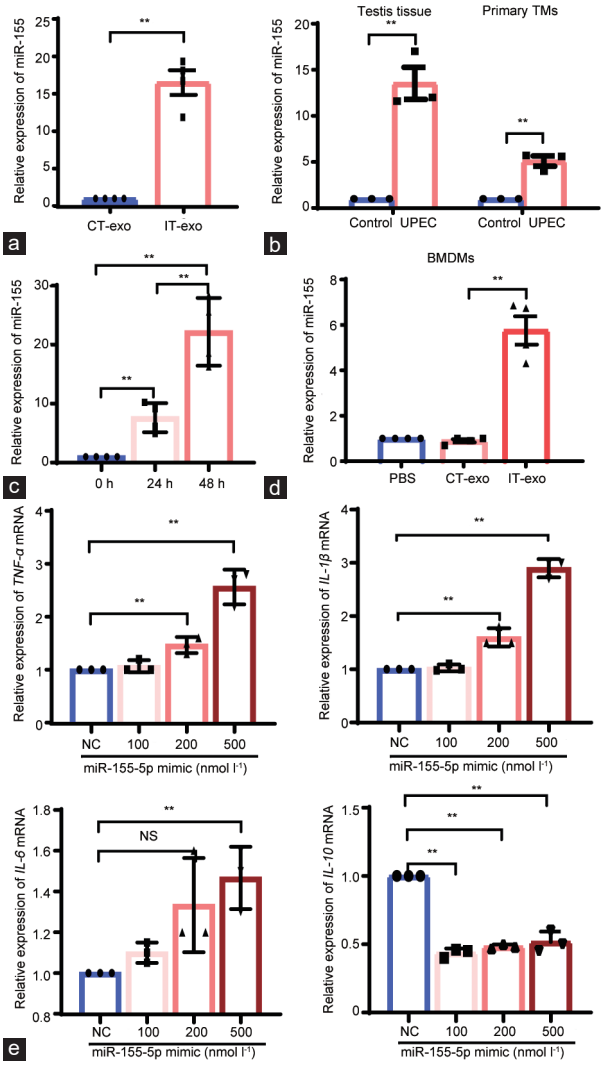

Figure 4: IT-exos-derived miR-155-5p facilitates macrophage polarization toward the proinflammatory phenotype. (**a**) The expression of miRNA-155-5p in testicular exosomes (n = 4 for each group). (**b**) The expression of miRNA-155-5p in testis tissue (n = 3) and primary TMs (n = 3) between the control group and the UPEC group. (**c**) The expression of miRNA-155-5p in BMDMs-derived M1 (induced by 100 ng ml^{-1} LPS and 50 ng ml^{-1} IFN-γ) at the indicated times (n = 4 for each group). (**d**) The expression of miRNA-155-5p in BMDMs after coculturing with different testicular exosomes for 48 h (exosomes 20 μg ml^{-1} or an equal volume of PBS as a negative control, n = 4 for each group). (**e**) The mRNA levels of M1-related genes (*TNF-α*, *IL-1β*, and *IL-6*) and an M2-related gene (*IL-10*) after transfecting miRNA NC or miR-155-5p mimic (100 nmol l^{-1}, 200 nmol l^{-1}, 500 nmol l^{-1}) into BMDMs (n = 3 for each group). All results are presented as the mean ± s.e.m. $^{*}P < 0.05$, $^{**}P < 0.01$. s.e.m.: standard error of mean; miRNA: micro ribonucleic acid; IT-exo: inflammatory testes-derived exosome; TM: testicular macrophage; UPEC: uropathogenic *Escherichia coli*; BMDM: bone marrow derived macrophage; LPS: lipopolysaccharide; INF-γ: interferon γ; PBS: phosphate buffered solution; *TNF-α*: tumor necrosis factor-α; mRNA: messenger ribonucleic acid; *IL-1β*: interleukin-1β; *IL-6*: interleukin-6; *IL-10*: interleukin-10; NC: negative control; CT-exo: control testes-derived exosome; NS: no significance.

impaired spermatogenesis that often accompanies bacterial orchitis. In contrast, mice treated with IT-exos encapsulating antagomiR-155 were less severely affected (**Figure 5j**). Taken together, the data indicated that IT-exo derived miR-155 plays an important role in disturbing testicular immune homeostasis during orchitis.

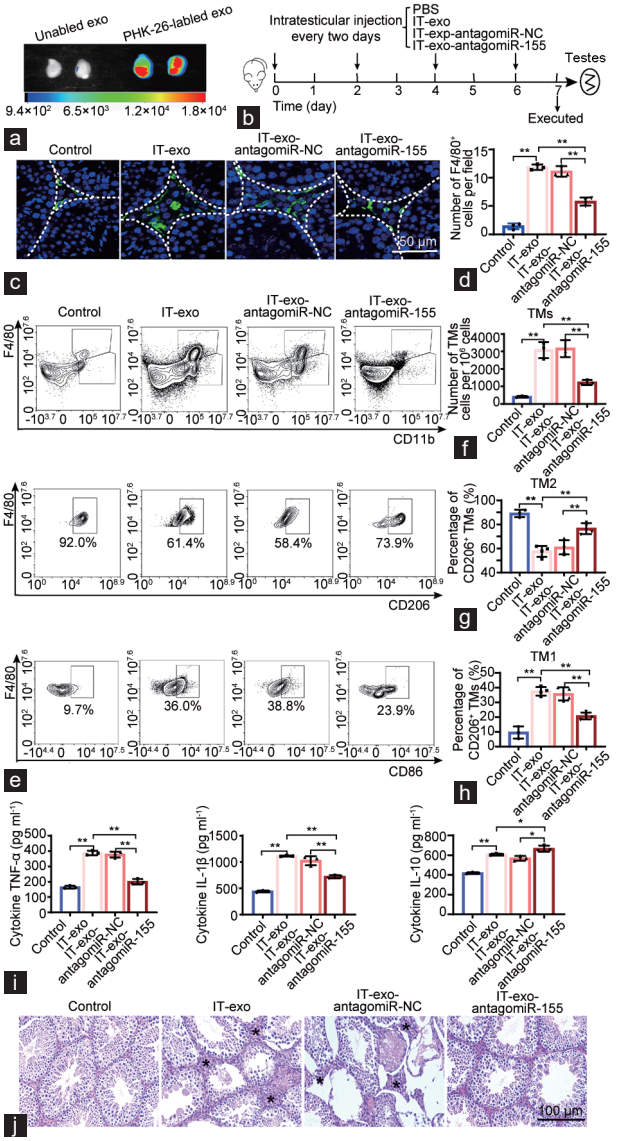

Figure 5: IT-exos disturbed the immunosuppressive phenotype of testicular macrophages, which was partially reversed by antagomiR-155 *in vivo*. (**a**) Bioluminescence imaging confirmed that IT-exos were retained within the testes by intratesticular injection of PKH-26-labeled IT-exos. (**b**) Protocol of exosome injection. The mice were injected with PBS, IT-exos, and IT-exos loaded with antagomiR-155 or the negative control at the indicated time courses. Approximately 10 μl of exosomes (1 μg μl^{-1} at the protein level) was injected into the testis every two days. (**c**) Representative immunofluorescence image of F4/80^{+} TMs (green) in different treatment groups as indicated. Scale bar = 50 μm. (**d**) Quantification of F4/80^{+} TM cells (numbers of per field, n = 3). (**e**) Representative flow cytometry plots of F4/80^{+}CD11b^{+} TMs (upper panel), F4/80^{+}CD11b^{+}CD206^{+} TM2 (middle panel), and F4/80^{+}CD11b^{+}CD86^{+} TM1 (lower panel) in testes in different groups are presented. (**f**) The number of F4/80^{+}CD11b^{+} TMs in the testes of different groups is presented (n = 3 for each group). (**g**) The percentage of CD206^{+} TM2 cells among F4/80^{+}CD11b^{+} TMs in different groups is shown (n = 4). (**h**) Percentage of CD86^{+} TM1 among F4/80^{+}CD11b^{+} TMs in different groups is shown (n = 4). (**i**) The secretion of proinflammatory cytokines TNF-α and IL-1β and the anti-inflammatory cytokine IL-10 in testes in different treatment groups as indicated (n = 3). (**j**) Testicular tissue sections from each treatment group were stained with hematoxylin and eosin. Scale bar = 100 μm. All results are presented as the mean ± s.e.m. $^{*}P < 0.05$, $^{**}P < 0.01$. s.e.m.: standard error of mean; PKH-26: Paul Karl Horan-26; IT-exo: inflammatory testes-derived exosome; PBS: phosphate buffered solution; TM: testicular macrophage; TNF-α: tumor necrosis factor-α; IL-1β: interleukin-1β; IL-10: interleukin-10.

DISCUSSION

Accumulating studies highlight the importance of testicular macrophages in maintaining testicular immune homeostasis.[15,35] It is also clear that macrophages with high plasticity, typically defined as M1 and M2, are highly influenced by microenvironmental signals including exosomes.[10,19,35] The present study demonstrated that IT-exos disturbed testicular immune homeostasis by facilitating the activation of TMs to an M1-like proinflammatory phenotype. Furthermore, we identified that the miR-155-5p transferred by IT-exos promoted the activation of proinflammatory M1 polarization in UPEC-induced orchitis. IT-exos encapsulating the miR-155 inhibitor reduced the inflammatory response, while they increased the levels of anti-inflammatory cytokines and M2 marker expression. Therapeutic targeting of IT-exos-miR-155-5p may be a new approach to govern inflammation and alleviate inflammation-related male infertility.

It has been reported that exosomes transfer biological information from their donor cells to receptor cells.[18] Many previous investigations have focused on the function of exosomes isolated from the culture medium of different cell lines, including fibroblasts,[41] adipocytes,[37] and mesenchymal stromal cells.[42] However, exosomes derived from cell models only represent a portion of the *in vivo* events. Therefore, tissue-derived exosomes obtained from a variety of body fluids are considered better research material. Given that testicular interstitial fluid is scarce and difficult to obtain, it is challenging to obtain testicular exosomes. A recent study demonstrated a reliable new method for testicular exosome extraction from the digestive fluid of testicular tissue.[32] In the present study, we successfully isolated IT-exos from the UPEC-induced orchitis mouse model by differential centrifugation.

Recent investigations showed that exosomes derived from inflammatory tissue induced increased expression of $F4/80^+CD11b^+$ macrophages, increased the percentage of $CD86^+$ M1 macrophages and decreased the proportion of $CD206^+$ M2 macrophages.[19,20] Zhang *et al*.[15] also reported that UPEC-induced orchitis was characterized by a higher number of $F4/80^+CD11b^+$ macrophages and a lower percentage of $CD206^+$ M2 macrophages than the sham control. In agreement with these findings, our data showed that IT-exos promoted the activation of M1-like macrophages with increased expression of CD86 in $F4/80^+CD11b^+$ primary TMs and decreased CD206 in $F4/80^+CD11b^+$ primary TMs. Furthermore, we demonstrated that IT-exos promoted TMs production of high levels of proinflammatory cytokines (TNF-α, IL-1β, and IL-6) by TMs *in vitro* and *in vivo*. These data revealed that IT-exos possessed potent abilities to induce testis inflammation. These results align with previous studies that have reported that inflammatory tissue-derived exosomes carry a cargo characteristic of that particular disease and mediate biological effects by inducing proinflammatory macrophage activation.[19,43] It is important to note that lymphocytes could also secrete proinflammatory cytokines under inflammatory conditions[44] and that there might be some changes in lymphocytes *in vivo*. In addition, we found that CT-exos have immunosuppressive properties *in vitro*, which is in agreement with the report that interstitial fluid surrounding the TM has an anti-inflammatory effect under physiological conditions.[4]

miRNAs can be transferred to the recipient cells over a long distance by exosomes, as exosomes provide a safe shuttle for miRNAs to prevent degradation during communication between the tissue microenvironment and receptor cells. For example, miR-192-5p derived from exosomes triggers M1 macrophages during the development of nonalcoholic fatty liver disease.[45] Moreover, exosomes derived from different tissues and cells tend to have distinct miRNA profiles.[46–48] The miRNAs that are transferred to recipient cells by exosomes are not random and may vary due to the different types of recipient cells.[38] In the present study, we identified several differentially expressed miRNAs encapsulated into IT-exos by small RNA sequencing. Of these miRNAs, miR-155-5p was one of the most highly enriched miRNAs in IT-exos. We further confirmed that the expression level of miR-155-5p was increased not only in IT-exos but also in UPEC-infected testis tissue or primary TMs derived from UPEC-infected testis. We also found that the level of miR-155-5p was upregulated in BMDMs stimulated with IT-exos. These data suggested that miR-155-5p capsuled into IT-exos may play a role in communication between the testicular microenvironment and TMs.

To better elucidate the function of miR-155-5p packed in IT-exos, we used an miR-155-5p mimic to confirm its role in the activation of macrophages. Ge *et al*.[19] reported that miR-155-5p was one of the top 10 highly expressed miRNAs in ischemia-reperfusion induced exosomes, which activate inflammatory response in the ischemia-reperfusion tissue. Similar to these studies, we found that the miR-155-5p mimic promoted the expression of proinflammatory cytokines. Recent studies also revealed that miR-155 promoted the inflammatory response by inhibiting suppressor of cytokine signaling 1 (SOCS1) and other anti-inflammatory genes.[19,49,50] It has been demonstrated that RNA interference (RNAi) is an efficient and key tool for manipulating genes with target-specificity.[51] Ma *et al*.[34] delivered of exosomes encapsulating antagomiR-182 targeted breast cancer, leading to miR-182 inhibition, macrophage reprogramming, and tumor suppression. Our *in vivo* experiments revealed that IT-exos-mediated antagomiR-155 reduced the number of $F4/80^+$ TMs and decreased the levels of proinflammatory cytokines, while it increased the expression of M2 marker genes in the testes. These results suggested that knockdown of miR-155-5p in IT-exos relieved testis inflammation and partially improved testicular immune privilege. Although we found that miR-155-5p delivered by IT-exos can activate M1-like macrophages, it should be noted that other biological molecules, such as long-noncoding RNAs, lipids, and proteins in IT-exos, may also take part in disturbing testicular immune homeostasis, which is not excluded.

CONCLUSIONS

IT-exos-miR-155-5p promoted the polarization of TMs to proinflammatory TM1 in inflamed testicular tissue. These findings improved our understanding of orchitis-induced immune disorders in testes and shed new light on the role of testicular exosomes in testicular inflammatory injury, supporting the therapeutic potential of targeting IT-exos-miR-155-5p in clinical settings.

AUTHOR CONTRIBUTIONS

JX designed and performed the experiments and wrote the manuscript. CH analyzed the data. YWF and ZYH performed the experiments. MLP, YYC, YFS and CYL contributed to read and revise the manuscript. HPZ and KZ conducted the experiments, figure preparation and manuscript drafting. All authors read and approved the final manuscript.

COMPETING INTERESTS

All authors declare no competing interests.

ACKNOWLEDGMENTS

This work was funded by National Key R&D Program of China (2018YFC1004300 and 2018YFC1004304), and National Natural Foundation of China (No. 81871148 and No. 818701539).

Supplementary Information is linked to the online version of the paper on the *Asian Journal of Andrology* website.

REFERENCES

1 Virtanen HE, Jørgensen N, Toppari J. Semen quality in the 21st century. *Nat Rev Urol* 2017; 14: 120–30.
2 Schuppe HC, Pilatz A, Hossain H, Diemer T, Wagenlehner F, *et al.* Urogenital infection as a risk factor for male infertility. *Dtsch Arztebl Int* 2017; 114: 339–46.
3 Isaiah IN, Nche BT, Nwagu IG, Nnanna II. Current studies on bacterospermia the leading cause of male infertility: a protégé and potential threat towards mans extinction. *N Am J Med Sci* 2011; 3: 562–4.
4 Wang M, Fijak M, Hossain H, Markmann M, Nüsing RM, *et al.* Characterization of the micro-environment of the testis that shapes the phenotype and function of testicular macrophages. *J Immunol* 2017; 198: 4327–40.
5 Fijak M, Meinhardt A. The testis in immune privilege. *Immunol Rev* 2006; 213: 66–81.
6 Fijak M, Pilatz A, Hedger MP, Nicolas N, Bhushan S, *et al.* Infectious, inflammatory and 'autoimmune' male factor infertility: how do rodent models inform clinical practice? *Hum Reprod Update* 2018; 24: 416–41.
7 Murray PJ. Macrophage polarization. *Annu Rev Physiol* 2017; 79: 541–66.
8 Bhushan S, Meinhardt A. The macrophages in testis function. *J Reprod Immunol* 2017; 119: 107–12.
9 Rival C, Theas MS, Suescun MO, Jacobo P, Guazzone V, *et al.* Functional and phenotypic characteristics of testicular macrophages in experimental autoimmune orchitis. *J Pathol* 2008; 215: 108–17.
10 Winnall WR, Hedger MP. Phenotypic and functional heterogeneity of the testicular macrophage population: a new regulatory model. *J Reprod Immunol* 2013; 97: 147–58.
11 Bhushan S, Tchatalbachev S, Lu Y, Fröhlich S, Fijak M, *et al.* Differential activation of inflammatory pathways in testicular macrophages provides a rationale for their subdued inflammatory capacity. *J Immunol* 2015; 194: 5455–64.
12 Winnall WR, Muir JA, Hedger MP. Rat resident testicular macrophages have an alternatively activated phenotype and constitutively produce interleukin-10 *in vitro*. *J Leukoc Biol* 2011; 90: 133–43.
13 Gerdprasert O, O'Bryan MK, Nikolic-Paterson DJ, Sebire K, de Kretser DM, *et al.* Expression of monocyte chemoattractant protein-1 and macrophage colony-stimulating factor in normal and inflamed rat testis. *Mol Hum Reprod* 2002; 8: 518–24.
14 Klein B, Bhushan S, Günther S, Middendorff R, Loveland KL, *et al.* Differential tissue-specific damage caused by bacterial epididymo-orchitis in the mouse. *Mol Hum Reprod* 2020; 26: 215–27.
15 Zhang Z, Jiang Z, Zhang Y, Zhang Y, Yan Y, *et al.* Corticosterone enhances the AMPK-mediated immunosuppressive phenotype of testicular macrophages during uropathogenic *Escherichia coli* induced orchitis. *Front Immunol* 2020; 11: 583276.
16 Pérez CV, Theas MS, Jacobo PV, Jarazo-Dietrich S, Guazzone VA, *et al.* Dual role of immune cells in the testis: protective or pathogenic for germ cells? *Spermatogenesis* 2013; 3: e23870.
17 Tkach M, Théry C. Communication by extracellular vesicles: where we are and where we need to go. *Cell* 2016; 164: 1226–32.
18 Colombo M, Raposo G, Théry C. Biogenesis, secretion, and intercellular interactions of exosomes and other extracellular vesicles. *Annu Rev Cell Dev Biol* 2014; 30: 255–89.
19 Ge X, Meng Q, Wei L, Liu J, Li M, *et al.* Myocardial ischemia-reperfusion induced cardiac extracellular vesicles harbour proinflammatory features and aggravate heart injury. *J Extracell Vesicles* 2021; 10: e12072.
20 Wei M, Gao X, Liu L, Li Z, Wan Z, *et al.* Visceral adipose tissue derived exosomes exacerbate colitis severity pro-inflammatory miRNAs in high fat diet fed mice. *ACS Nano* 2020; 14: 5099–110.
21 Yan C, Zhou QY, Wu J, Xu N, Du Y, *et al.* Csi-let-7a-5p delivered by extracellular vesicles from a liver fluke activates M1-like macrophages and exacerbates biliary injuries. *Proc Natl Acad Sci U S A* 2021; 118: e2102206118.
22 Wang Y, Liang H, Jin F, Yan X, Xu G, *et al.* Injured liver-released miRNA-122 elicits acute pulmonary inflammation via activating alveolar macrophage TLR7 signaling pathway. *Proc Natl Acad Sci U S A* 2019; 116: 6162–71.
23 Frenette G, Lessard C, Madore E, Fortier MA, Sullivan R. Aldose reductase and macrophage migration inhibitory factor are associated with epididymosomes and spermatozoa in the bovine epididymis. *Biol Reprod* 2003; 69: 1586–92.
24 Pons-Rejraji H, Artonne C, Sion B, Brugnon F, Canis M, *et al.* Prostasomes: inhibitors of capacitation and modulators of cellular signalling in human sperm. *Int J Androl* 2011; 34: 568–80.
25 Siciliano L, Marcianò V, Carpino A. Prostasome-like vesicles stimulate acrosome reaction of pig spermatozoa. *Reprod Biol Endocrinol* 2008; 6: 5.
26 Zhou W, Stanger SJ, Anderson AL, Bernstein IR, De Iuliis GN, *et al.* Mechanisms of tethering and cargo transfer during epididymosome-sperm interactions. *BMC Biol* 2019; 17: 35.
27 Welch RA, Burland V, Plunkett G, Redford P, Roesch P, *et al.* Extensive mosaic structure revealed by the complete genome sequence of uropathogenic *Escherichia coli*. *Proc Natl Acad Sci U S A* 2002; 99: 17020–4.
28 Li Y, Su Y, Zhou T, Hu Z, Wei J, *et al.* Activation of the NLRP3 inflammasome pathway by prokineticin 2 in testicular macrophages of uropathogenic *Escherichia coli*-induced orchitis. *Front Immunol* 2019; 10: 1872.
29 Ying W, Cheruku PS, Bazer FW, Safe SH, Zhou B. Investigation of macrophage polarization using bone marrow derived macrophages. *J Vis Exp* 2013; 76: 50323.
30 Wang M, Yang Y, Cansever D, Wang Y, Kantores C, *et al.* Two populations of self-maintaining monocyte-independent macrophages exist in adult epididymis and testis. *Proc Natl Acad Sci U S A* 2021; 118: e2013686117.
31 Martin E, El-Behi M, Fontaine B, Delarasse C. Analysis of microglia and monocyte-derived macrophages from the central nervous system by flow cytometry. *J Vis Exp* 2017; 124: 55781.
32 Crescitelli R, Lässer C, Lötvall J. Isolation and characterization of extracellular vesicle subpopulations from tissues. *Nat Protoc* 2021; 16: 1548–80.
33 Rajasekaran S, Thatte J, Periasamy J, Javali A, Jayaram M, *et al.* Infectivity of adeno-associated virus serotypes in mouse testis. *BMC Biotechnol* 2018; 18: 70.
34 Ma C, He D, Tian P, Wang Y, He Y, *et al.* miR-182 targeting reprograms tumor-associated macrophages and limits breast cancer progression. *Proc Natl Acad Sci U S A* 2022; 119: e2114006119.
35 Meinhardt A, Wang M, Schulz C, Bhushan S. Microenvironmental signals govern the cellular identity of testicular macrophages. *J Leukoc Biol* 2018; 104: 757–66.
36 Zhou J, Liu W, Zhao X, Xian Y, Wu W, *et al.* Natural melanin/alginate hydrogels achieve cardiac repair through ROS scavenging and macrophage polarization. *Adv Sci (Weinh)* 2021; 8: e2100505.
37 Pan Y, Hui X, Hoo RLC, Ye D, Chan CY, *et al.* Adipocyte-secreted exosomal microRNA-34a inhibits M2 macrophage polarization to promote obesity-induced adipose inflammation. *J Clin Invest* 2019; 129: 834–49.
38 Garcia-Martin R, Wang G, Brandão BB, Zanotto TM, Shah S, *et al.* MicroRNA sequence codes for small extracellular vesicle release and cellular retention. *Nature* 2021; 601: 446–51.
39 Vigorito E, Kohlhaas S, Lu D, Leyland R. miR-155: an ancient regulator of the immune system. *Immunol Rev* 2013; 253: 146–57.
40 Fitzsimons S, Oggero S, Bruen R, McCarthy C, Strowitzki MJ, *et al.* microRNA-155 is decreased during atherosclerosis regression and is increased in urinary extracellular vesicles during atherosclerosis progression. *Front Immunol* 2020; 11: 576516.
41 Bang C, Batkai S, Dangwal S, Gupta SK, Foinquinos A, *et al.* Cardiac fibroblast-derived microRNA passenger strand-enriched exosomes mediate cardiomyocyte hypertrophy. *J Clin Invest* 2014; 124: 2136–46.
42 Morrison TJ, Jackson MV, Cunningham EK, Kissenpfennig A, McAuley DF, *et al.* Mesenchymal stromal cells modulate macrophages in clinically relevant lung injury models by extracellular vesicle mitochondrial transfer. *Am J Respir Crit Care Med* 2017; 196: 1275–86.
43 Saha B, Momen-Heravi F, Furi I, Kodys K, Catalano D, *et al.* Extracellular vesicles from mice with alcoholic liver disease carry a distinct protein cargo and induce macrophage activation through heat shock protein 90. *Hepatology* 2018; 67: 1986–2000.
44 Bhushan S, Theas MS, Guazzone VA, Jacobo P, Wang M, *et al.* Immune cell subtypes and their function in the testis. *Front Immunol* 2020; 11: 583304.
45 Liu XL, Pan Q, Cao HX, Xin FZ, Zhao ZH, *et al.* Lipotoxic hepatocyte-derived exosomal microRNA 192-5p activates macrophages through Rictor/Akt/Forkhead box transcription factor O1 signaling in nonalcoholic fatty liver disease. *Hepatology* 2020; 72: 454–69.
46 Martens-Uzunova ES, Kusuma GD, Crucitta S, Lim HK, Cooper C, *et al.* Androgens alter the heterogeneity of small extracellular vesicles and the small RNA cargo in prostate cancer. *J Extracell Vesicles* 2021; 10: e12136.
47 Wang X, Wilkinson R, Kildey K, Ungerer JP, Hill MM, *et al.* Molecular and functional profiling of apical versus basolateral small extracellular vesicles derived from primary human proximal tubular epithelial cells under inflammatory conditions. *J Extracell Vesicles* 2021; 10: e12064.
48 Sun P, Wang N, Zhao P, Wang C, Li H, *et al.* Circulating exosomes control $CD4^+$ T cell immunometabolic functions via the transfer of miR-142 as a novel mediator in myocarditis. *Mol Ther* 2020; 28: 2605–20.
49 Huffaker TB, O'Connell RM. miR-155-SOCS1 as a functional axis: satisfying the burden of proof. *Immunity* 2015; 43: 3–4.
50 Baig MS, Zaichick SV, Mao M, de Abreu AL, Bakhshi FR, *et al.* NOS1-derived nitric oxide promotes NF-κB transcriptional activity through inhibition of suppressor of cytokine signaling-1. *J Exp Med* 2015; 212: 1725–38.
51 Anandanarayanan A, Raina OK, Lalrinkima H, Rialch A, Sankar M, *et al.* RNA interference in *Fasciola gigantica*: establishing and optimization of experimental RNAi in the newly excysted juveniles of the fluke. *PLoS Negl Trop Dis* 2017; 11: e0006109.

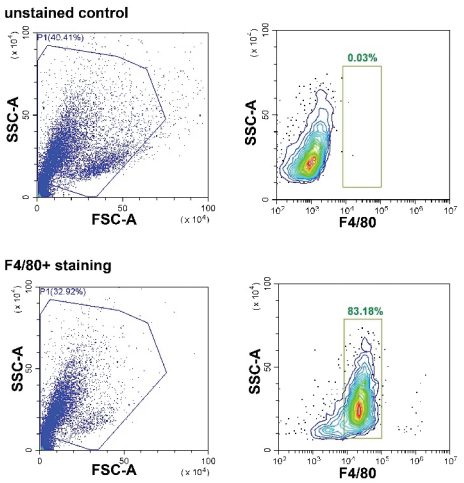

Supplementary Figure 1: The purity of primary TMs (8–9 weeks, $n = 4$ per group) was verified using F4/80 antibody (BV421-F4/80, eBioscience, 48-4801-82). TM: testicular macrophage.

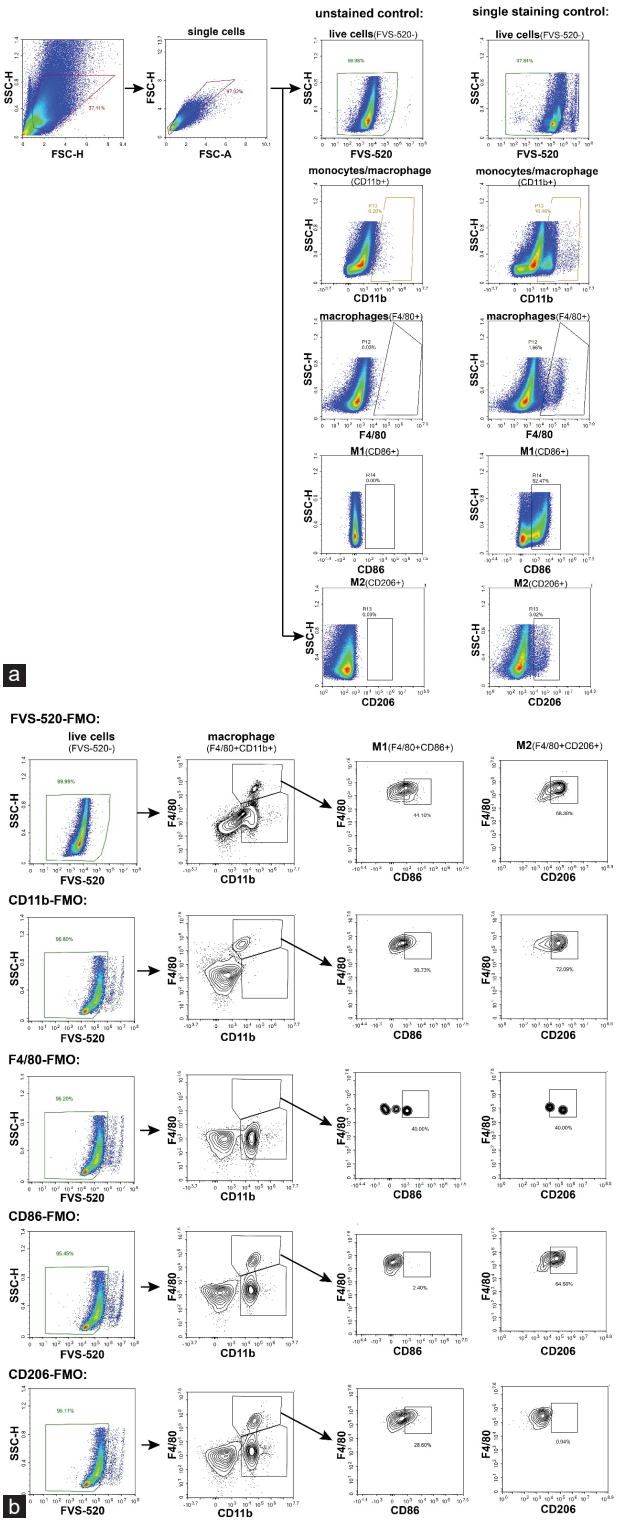

Supplementary Figure 2: The single staining fluorescence control (**a**) and FMO control (**b**) of each fluorescent marker in **Figure 1D** and **Figure 5E** (8–9 weeks, $n = 2$). FMO: fluorescence minus one.

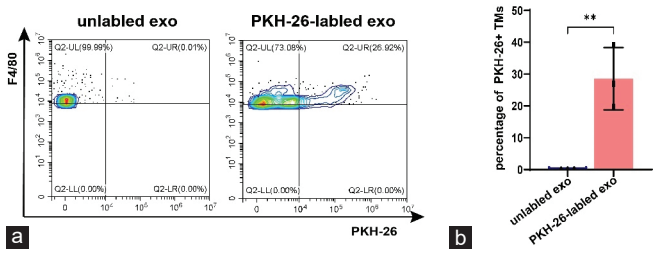

Supplementary Figure 3: The percentage of PKH-26$^+$ TMs (8 weeks, $n = 3$ per group) was verified using flow cytometry. (**a**) Representative flow cytometry plotes of PKH-26$^+$ TM. (**b**) The percentage of PKH-26$^+$ TM ($n = 3$). The results are presented as mean ± s.e.m. $^{**}P < 0.01$. PKH-26: Paul Karl Horan-26; TM: testicular macrophage; s.e.m.: standard error of mean.

SUPPLEMENTARY METHODS AND MATERIALS

THE METHOD OF TMS TAKE UP IT-EXO *IN VIVO*

We have analyzed the TM take up IT-exos *in vivo*: Adult mice were anesthetized and approximately 10 μl of PKH26-labeled exosomes (10 μg per 10 μl at protein level) was injected bilaterally into the testis. Sham operated mice were injected with the equal volume of unlabeled exosomes. After 24 h, the mice were sacrificed, the testis were removed, and washed with pre-cold PBS and then were decapsulated and digested in DMEM/F12 medium containing 1 mg ml^{-1} collagenase I (sigma, USA) and DNase I (Sigma, 60 U ml^{-1}) at 34°C for 15 min. Then, the digestive solution was filtered to separate the interstitial cells and seminiferous tubules. After centrifugating the suspension, the pellet containing interstitial cells were resuspended and purified with a discontinuous density percoll (GE Healthcare, 17-0891-09) solution. After centrifugating, the relevant interphase containing immune cells was collected and washed with PBS; the single-cell suspension of testicular interstitial immune cells was obtained. For detecting the percentage of PKH-26^+ TMs, the testicular interstitial immune cells were incubated with flow cytometry antibodies, including BV510 (BD, 564406), and BV421-F4/80 (eBioscience, 48-4801-82) at 4°C in the dark for 30 min, cells were washed and resuspended in PBS buffer containing 1% BSA. After that, flow cytometry was performed.

Supplementary Table 1: Primers used in the real-time polymerase chain reaction assays

Gene	*Primer sequences (5′–3′)*
mmu-miR-155-5p	
Stem loop primers	CCTGTTGTCTCCAGCCACAAAAGAGCACAATATTTCAGGAGACAACAGG
Forward	CGGGCTTAATGCTAATTGTGA
Reverse	CAGCCACAAAAGAGCACAAT
mus-U6	
Forward	CTCGCTTCGGCAGCACATATACT
Reverse	ACGCTTCACGAATTTGCGTGTC
mus-TNF-α	
Forward	CTGAACTTCGGGGTGATCGG
Reverse	GGCTTGTCACTCGAATTTTGAGA
mus-IL-1β	
Forward	GAAATGCCACCTTTTGACAGTG
Reverse	TGGATGCTCTCATCAGGACAG
mus-IL-6	
Forward	CTGCAAGAGACTTCCATCCAG
Reverse	AGTGGTATAGACAGGTCTGTTGG
mus-IL-10	
Forward	GCTCTTACTGACTGGCATGAG
Reverse	CGCAGCTCTAGGAGCATGTG
mus-GAPDH	
Forward	AAGAAGGTGGTGAAGCAGG
Reverse	GAAGGTGGAAGAGTGGGAGT

TNF-α: tumor necrosis factor-α; IL-6: interleukin-6; U6: uracil 6; GAPDH: glyceraldehyde-3-phosphate dehydrogenase; IL-1β: interleukin-1β; IL-10: interleukin-10

Supplementary Table 2: Differentially expressed micro-RNAs in inflammatory testes-derived exosomes (control *vs* uropathogenic *Escherichia coli*)

ID	*Base mean*	*Log2 fold change*	*P*	*P adjusted*	*Direction*
mmu-miR-142a-5p	307.2386559	3.72408093	5.32682E-17	2.59416E-14	Up
mmu-miR-142a-3p	162.861265	2.749099095	5.77378E-16	1.40592E-13	Up
mmu-miR-21a-5p	27713.11572	2.343223295	8.5781E-13	1.39251E-10	Up
mmu-miR-223-3p	72.61552736	3.512260908	5.63585E-12	6.86164E-10	Up
mmu-miR-451a	69.78392947	4.09331615	7.77826E-10	7.57603E-08	Up
mmu-miR-155-5p	82.60032438	3.374824883	1.8072E-09	1.46685E-07	Up
mmu-miR-468-3p	225.2876981	–2.226024738	6.78162E-09	4.71807E-07	Down
mmu-miR-6240	130.2779043	–1.923568006	5.61647E-08	3.41903E-06	Down
mmu-miR-146a-5p	2886.518406	1.511248037	2.08762E-07	1.12963E-05	Up
mmu-miR-223-5p	26.24127205	3.786621184	1.98668E-06	9.67513E-05	Up
mmu-miR-669c-5p	404.7788086	–1.694912595	3.92571E-06	0.000173802	Down
mmu-miR-7210-3p	165.0517538	–1.565186354	1.50979E-05	0.000612724	Down
mmu-miR-139-5p	50.36039241	2.123634479	4.31357E-05	0.001615928	Up
mmu-miR-19b-3p	825.6855698	1.284594488	7.77914E-05	0.002706031	Up
mmu-miR-542-3p	343.6067525	1.140371418	0.000126604	0.004110425	Up
mmu-miR-146b-5p	352.2963773	1.343779739	0.000140213	0.004267732	Up
mmu-miR-450b-5p	52.03630409	1.587664399	0.000186052	0.005329856	Up
mmu-miR-7230-3p	117.7915156	–1.283250304	0.00023823	0.006445459	Down
mmu-miR-5099	715.9137212	–1.3282809	0.000378777	0.009323874	Down
mmu-let-7f-5p	8167.023796	–1.051484679	0.000382911	0.009323874	Down
mmu-miR-132-3p	39.84830813	1.90109908	0.000538922	0.011226591	Up
mmu-miR-122-5p	17.18193257	–1.980612281	0.000553261	0.011226591	Down
mmu-miR-27b-5p	3.236344902	–5.412955377	0.000621055	0.012098151	Down
mmu-miR-486b-5p	43.35761129	2.191005557	0.000839476	0.015724037	Up
mmu-miR-12182-3p	24.75529166	–1.750723857	0.000930542	0.016784227	Down
mmu-miR-222-3p	30.50023767	1.58964564	0.001002251	0.016882237	Up
mmu-miR-486a-5p	43.05800206	2.17882671	0.001005308	0.016882237	Up
mmu-miR-147-3p	448.9796427	1.366301913	0.001117012	0.018132823	Up
mmu-miR-468-5p	1653.054289	–1.284166891	0.001249858	0.019634861	Down
mmu-miR-140-3p	903.3881342	1.684605987	0.001506079	0.022920638	Up
mmu-miR-20a-5p	1142.225805	1.040823293	0.002033241	0.028291096	Up
mmu-miR-21a-3p	8.239057941	2.62352239	0.0028363	0.038076148	Up
mmu-miR-217-5p	11.3774053	2.663089539	0.002892849	0.038076148	Up
mmu-miR-10a-5p	1569.410488	1.147838268	0.003019878	0.038702121	Up
mmu-miR-671-5p	10.45864241	–2.166685203	0.004096123	0.0498703	Down
mmu-miR-30b-3p	25.2586548	–1.311267641	0.006199797	0.067978428	Down
mmu-miR-7242-5p	2.921834953	–4.225187946	0.008124052	0.084179007	Down
mmu-miR-7222-5p	8.852372641	–1.890369129	0.00987989	0.096356538	Down
mmu-miR-148a-3p	152944.9453	–1.033922665	0.009988027	0.096356538	Down
mmu-miR-669a-5p	43.61362277	–1.05117758	0.010288583	0.096356538	Down
mmu-miR-1198-5p	19.30726771	1.374823493	0.011943373	0.105753143	Up
mmu-miR-3471	4.130365588	–3.054049268	0.01332515	0.115881218	Down
mmu-miR-5114	2.493593451	–3.993147394	0.013927176	0.118991838	Down
mmu-miR-206-3p	2.595474079	–4.01100576	0.016023028	0.132257876	Down
novel-miR-18_21490-5p	4.715944342	–2.52109166	0.016858932	0.133685885	Down
novel-miR-X_23093-5p	4.715944342	–2.52109166	0.016858932	0.133685885	Down
mmu-miR-484	6.850941796	2.242293715	0.017429949	0.133685885	Up
mmu-miR-200b-5p	11.30152248	1.633829499	0.017891795	0.133685885	Up
mmu-miR-7233-3p	29.07496046	–1.104998308	0.0180036	0.133685885	Down
mmu-miR-144-3p	3.615707806	3.075319567	0.028403206	0.200469007	Up
mmu-miR-331-3p	2.734032171	3.603196542	0.029970306	0.204062167	Up
mmu-miR-377-3p	1.414706444	–4.200634593	0.030019191	NA	Down
mmu-miR-7689-3p	3.461879646	3.019334751	0.03012273	0.204062167	Up
mmu-miR-126a-5p	33.01182036	1.068253357	0.03355923	0.220856017	Up
mmu-miR-409-5p	2.346837141	3.365582339	0.037678933	0.241442637	Up
mmu-miR-32-3p	5.132302854	–1.999360112	0.042072983	0.260626973	Down
mmu-miR-496a-3p	11.08317951	–1.393417161	0.042309189	0.260626973	Down

NA: not available

Supplementary Table 3: Differentially expressed micro-RNAs in primary testicular macrophages (control *vs* uropathogenic *Escherichia coli*)

ID	*Base mean*	*Log2 fold change*	*P*	*P adjusted*	*Direction*
mmu-miR-21a-5p	208778.2998	3.564172777	6.9187E-207	3.3071E-204	Up
mmu-miR-142a-3p	1080.634458	3.201597172	1.3461E-103	3.2171E-101	Up
mmu-miR-142a-5p	879.6668606	3.353452403	2.81378E-85	4.48328E-83	Up
mmu-miR-146a-5p	5858.270602	2.787860662	1.19496E-81	1.42798E-79	Up
mmu-miR-155-5p	213.2083209	4.478053721	2.52791E-63	2.41669E-61	Up
mmu-miR-223-3p	231.7432802	3.07303235	2.86686E-47	2.28393E-45	Up
mmu-miR-150-5p	184.6822665	2.831475955	4.30452E-41	2.93937E-39	Up
mmu-miR-378a-3p	2163.749618	1.445085963	2.13821E-33	1.27758E-31	Up
mmu-miR-223-5p	224.2260333	2.636121348	7.15316E-32	3.79912E-30	Up
mmu-miR-146b-5p	880.9883603	1.723410111	1.00764E-30	4.81653E-29	Up
mmu-miR-139-5p	419.6307415	1.564490715	3.56563E-23	1.54943E-21	Up
mmu-let-7i-5p	34392.08912	1.420929113	1.75329E-19	6.98393E-18	Up
mmu-miR-21a-3p	47.25145464	4.486098298	2.35329E-19	8.65285E-18	Up
mmu-miR-27a-5p	263.8384202	1.539813665	1.44986E-17	4.95022E-16	Up
mmu-let-7j	1248.020862	1.382921311	1.51645E-16	4.83242E-15	Up
mmu-miR-221-5p	77.12598334	2.363174016	1.31354E-15	3.69337E-14	Up
mmu-miR-27a-3p	2279.670094	1.193198861	8.2631E-15	2.19431E-13	Up
mmu-miR-221-3p	115.5633477	1.820569813	7.19955E-14	1.81126E-12	Up
mmu-miR-361-3p	468.3628984	1.143102988	8.4805E-14	2.02684E-12	Up
mmu-miR-222-3p	110.3018692	2.198535234	2.06138E-13	4.6921E-12	Up
mmu-miR-16-1-3p	392.7671092	1.103130819	1.59736E-12	3.47063E-11	Up
mmu-miR-210-3p	169.2914357	1.257496989	8.96177E-11	1.78489E-09	Up
mmu-miR-5099	3248.406039	1.131148045	2.45359E-09	4.69127E-08	Up
mmu-miR-378c	153.1362772	1.17101702	6.55675E-09	1.16079E-07	Up
mmu-miR-6240	28.72686629	3.107651671	8.27913E-09	1.41337E-07	Up
mmu-miR-363-3p	17.16317933	3.555115189	6.41282E-08	1.05701E-06	Up
mmu-miR-1198-5p	152.1732022	1.104907822	1.08846E-06	1.62589E-05	Up
mmu-miR-217-5p	20.41436408	2.355634742	3.16635E-06	4.20421E-05	Up
mmu-miR-7649-5p	7.347423087	6.292920592	3.38279E-06	4.3702E-05	Up
mmu-miR-484	42.39441735	1.353506422	5.63664E-05	0.000598736	Up
mmu-miR-7676-3p	10.11011236	3.848550847	6.92303E-05	0.000704087	Up
mmu-miR-222-5p	16.1110847	2.192656534	9.30475E-05	0.000907688	Up
mmu-miR-20b-5p	12.11315321	2.485710214	0.00017398	0.001599279	Up
mmu-miR-7043-3p	16.41190038	2.124351399	0.00024897	0.002163776	Up
mmu-miR-1964-3p	45.1360196	1.325685862	0.000498714	0.003844921	Up
mmu-miR-106a-5p	5.347913068	3.926009501	0.002340684	0.015119552	Up
novel-miR-6_11826-3p	8.552234567	2.225142703	0.003018702	0.017814069	Up
mmu-miR-155-3p	4.270962285	3.583233344	0.007622067	NA	Up
mmu-miR-574-5p	49.17395721	1.054184777	0.010344323	0.051443368	Up
mmu-miR-879-5p	1.853249035	–4.38905812	0.011087606	NA	Down
mmu-miR-378b	6.907082142	2.051428786	0.01204488	0.05703665	Up
mmu-miR-2137	4.286637934	2.898293651	0.01372315	NA	Up
mmu-miR-7229-3p	20.89318791	–1.145208438	0.013851383	0.063663089	Down
mmu-miR-362-5p	24.96308939	1.021247432	0.018734008	0.080674378	Up
mmu-miR-27b-5p	14.13577235	1.233749427	0.021512315	0.088645574	Up
mmu-miR-1936	1.595258272	4.089684683	0.022445811	NA	Up
mmu-miR-6537-3p	2.474576821	3.632207484	0.02248558	NA	Up
mmu-miR-150-3p	3.442884426	3.096570748	0.023604067	NA	Up
mmu-miR-301a-3p	21.36162783	1.14245722	0.02504138	0.099541983	Up
mmu-miR-495-3p	14.35454917	1.193328812	0.029362656	0.111391661	Up
mmu-miR-1930-5p	1.591441826	–4.156574663	0.032296042	NA	Down
mmu-miR-342-5p	14.27831421	1.132601966	0.03717578	0.135016686	Up
mmu-miR-219a-1-3p	6.340728024	1.755887419	0.041430102	0.148899162	Up
mmu-miR-18b-5p	3.487464698	2.537297	0.041876157	NA	Up
mmu-miR-344-3p	3.481616906	2.619209808	0.042773153	NA	Up
mmu-miR-301b-3p	5.720127124	1.745705177	0.048129372	0.165509638	Up
mmu-miR-3964	1.281999378	3.773154848	0.049642726	NA	Up

NA: not available

Supplementary Table 4: Differentially expressed micro-RNAs both in primary testicular macrophages (control *vs* uropathogenic *Escherichia coli*) and inflammatory testes-derived exosomes (control *vs* uropathogenic *Escherichia coli*)

Number	*ID*
1	mmu-miR-142a-5p
2	mmu-miR-146a-5p
3	mmu-miR-155-5p
4	mmu-miR-21a-3p
5	mmu-miR-223-3p
6	mmu-miR-142a-3p
7	mmu-miR-217-5p
8	mmu-miR-139-5p
9	mmu-miR-1198-5p
10	mmu-miR-21a-5p
11	mmu-miR-222-3p
12	mmu-miR-5099
13	mmu-miR-484
14	mmu-miR-223-5p
15	mmu-miR-27b-5p
16	mmu-miR-146b-5p
17	mmu-miR-6240